Experimental and computational assessment of U Si N ternary phases

Lopes, D.A.; Wilson, T.L.; Kocevski, V.; Moore, E.E.; Besman, T.M.; Wood, E. Sooby; White, J.T.; Nelson, A.T.; Middleburgh, Simon; Claisse, A.

Journal of Nuclear Materials

Published: 01/04/2019

Peer reviewed version

Accepted Manuscript

Experimental and computational assessment of U—Si—N ternary phases

D.A. Lopes, T.L. Wilson, V. Kocevski, E.E. Moore, T.M. Besmann, E. Sooby Wood, J.T. White, A.T. Nelson, S.C. Middleburgh, A. Claisse

PII: S0022-3115(18)31227-3

DOI: https://doi.org/10.1016/j.jnucmat.2019.01.008

Reference: NUMA 51391

To appear in: *Journal of Nuclear Materials*

Received Date: 5 September 2018

Revised Date: 12 December 2018

Accepted Date: 3 January 2019

Please cite this article as: D.A. Lopes, T.L. Wilson, V. Kocevski, E.E. Moore, T.M. Besmann, E. Sooby Wood, J.T. White, A.T. Nelson, S.C. Middleburgh, A. Claisse, Experimental and computational assessment of U—Si—N ternary phases, *Journal of Nuclear Materials* (2019), doi: https://doi.org/10.1016/j.jnucmat.2019.01.008.

Experimental and Computational Assessment of U-Si-N Ternary Phases

D. A. Lopes[1,2], T. L. Wilson[1], V. Kocevski[1], E. E. Moore[1], and T. M. Besmann[1]

1 -University of South Carolina

2 - *KTH-Royal Institute of Technology, Stockholm, Sweden*

E. Sooby Wood[3]

3- The University of Texas at San Antonio

J. T. White[4] and A. T. Nelson[4]

4-Los Alamos National Laboratory

S.C. Middleburgh[5,6] and A. Claisse[5,2]

5-Westinghouse Electric Sweden, AB

6-Nuclear Futures Institute, Bangor University, Bangor, LL57 1UT, U.K.

Uranium nitride-silicide composites are being considered as a high-density and high thermal conductivity fuel option for light water reactors. During development, chemical interactions were observed near the silicide melting point which resulted in formation of an unknown U-Si-N ternary phase. In the present work, U-Si-N composite samples were produced by arc-melting U_3Si_2 under an argon-nitrogen atmosphere to form the ternary phase. The resulting samples were characterized by SEM/EDS-EPMA and XRD, and demonstrated an equilibrium between U_3Si_2, UN, USi and a U-Si-N phase with a distinct crystallographic structure. Rietveld refinement of the ternary structure was performed, considering the ternary structures existent in the analogue U-Si-C system, and a good fit was obtained for the hexagonal $U_{20}Si_{16}N_3$ phase. DFT+*U* calculations were performed in parallel to evaluate the thermodynamic and dynamic stability of the ternaries $U_{20}Si_{16}N_3$ and $U_3Si_2N_2$. The calculated enthalpy of formation and phonon dispersion support the existence of stable $U_{20}Si_{16}N_3$ and $U_3Si_2N_2$, although some soft modes in the $U_{20}Si_{16}N_3$ phase phonons are observed. The results presented here thus demonstrate the occurrence of at least one ternary phase in the U-Si-N system.

1. Introduction

The Fukushima-Daiichi accident highlighted that even redundant safety systems in place for GEN-II reactors can simultaneously fail with serious consequences [1, 2]. Consequently, a drive to design fuel elements for light water reactors (LWRs), and especially the existing fleet of GEN II reactors, that have a more delayed and less damaging response to a major failure, such as a sustained loss of coolant or overpower-type accident, has gained a great deal of momentum. The result have been international efforts to develop more robust fuel-cladding systems. In the U. S. the Accident Tolerant Fuel (ATF) initiative aims to design a fuel element that can reduce oxidation kinetics, heat of oxidation in steam, and release of hydrogen [3]. Within these criteria new materials for cladding and fuel are being considered to replace the current Zr-UO_2 system [4,5]. Among the fuel materials are UN, U_3Si_2 and the composite UN/U_3Si_2 [6]. These compounds are being considered mainly due to their combination of high fissile density, high thermal conductivity and intermediated melting point. In particular, it is their increased uranium atom density over UO_2 of the which is the key factor, allowing replacement of Zr-alloy cladding with less reactive materials (such as FeCrAl and Mo alloys) while minimizing overall neutronic penalty.

Historical interest in UN for fuel applications is due to its good physical properties and acceptable behavior under irradiation [7], however, notable drawbacks include difficulty sintering as well as the cost penalty associated with the enrichment of ^{15}N, which is necessary to prevent ^{14}C generation by ^{14}N neutron absorption. Significant susceptibility to air and steam oxidation has also prevented its application in LWRs [8, 9, 10]. Although U_3Si_2 has been used for many years as a fuel in research reactors, its configuration in Al dispersed form and low temperature application, leads to a significant gap of knowledge for LWR application. [11]. Its high fissile density and thermal conductivity, and its moderate resistance to steam degradation (in comparison with UN compound) motivated its consideration as an ATF fuel. A concern is its lower melting point,1938 K, as compared with the 3130 K for UO_2 and 3120 K for UN [12], although it is speculated that its higher thermal conductivity should reduce the operating centerline temperature, still yielding a larger margin to melt. However, persisting issues to be addressed before U_3Si_2 becomes a viable LWR fuel are the high pulverization in steam and

pressurized water reactions (above 400^{o}C) [13, 14], and the lack of data concerning irradiation behavior under LWR conditions i.e., at high temperature and in monolithic/pellet form.

A UN/U_3Si_2 composite fuel (10-40 vol.% U_3Si_2) has recently been recommended to deal with some of the aforementioned issues [15,16,17]. The central concept for this composite fuel is to combine the better U_3Si_2 pulverization resistance in an oxidation atmosphere, with the high fissile density of UN. To accomplish this goal the desired microstructure consists of a matrix of UN grains covered by with U_3Si_2, has been proposed.

Despite being of more recent interest, the initial concept for the UN/U_3Si_2 composite fuel was developed in the early 1960's [16-18] , with the goal to improve the sintering of UN. The composite fuel was proposed as an alternative for required very high sintering temperatures of UN, where the UN/U_3Si_2 combination takes advantage of liquid-phase sintering fostered by the U_3Si_2, achieving suitable densities at T < 1600 °C. In this way the benefit of the composite is twofold, it is designed to be more resistance to pulverization, and the fabrication process is made easier. In the ATF initiative, the aim is to protect UN from oxygen/steam reactions by establishing grain-scale coating of U_3Si_2 [15, 19], yielding a 17-40% higher uranium density compared to UO_2, and a high melting point.

Initial reports of the so far limited efforts on UN/U_3Si_2 have shown that the addition of 25-35vol.% U_3Si_2 has allowed production of compacts of 89-94% of theoretical density (TD) in conventional sintering at 1700 ^{o}C [15]This compares to the 1900-2000 ^{o}C required to achieve the same density for solely UN [9]. Despite these promising results, evidence of reaction between UN and U_3Si_2 was detected, suggesting the formation of an as-yet unidentified ternary U-Si-N phase [15, 16]. The composition of the ternary phase has been hard to assess due to the large error associated with energy-dispersive X-ray spectroscopy (EDS) when heavy and light elements are simultaneously present, in this case, uranium and nitrogen. The uncertainty concerning the nature of the possible ternary phase makes its potential impact on fuel performance unclear, and thus prompts the investigation of a U-Si-N phase equilibria as it relates to the development of composite fuels for LWR's.

Modeling can also help to assess the composition of this ternary phase, and its stability. Although no density functional theory (DFT) studies of the U-N-Si exist, the work on nitride and silicide system can be readily used. In particular, for UN, the works of Gryaznov et al. [20]

establishing a reference *U*-value and of Claisse et al. [21] showing that metastable states are an issue are of interest, while on the silicide phase, the work of Noordhoek et al. [22] giving a *U*-valuer correction for U_3Si_2 can be used. Since it has been shown that the work done on U-Si-C could be used as a basis for U-Si-B and U-Si-Pt [23], the DFT study on $U_3Si_2C_2$ [24] is also worth mentioning.

In this study we synthesized ternary phase material by arc-melting U_3Si_2 in an argon-nitrogen atmosphere. This method has been successfully used in the past with uranium metal [25] and has the advantage of promoting fast diffusion of nitrogen in the liquid. The aim of this technique is to increase the amount of ternary phase formed, as compared with that seen in high temperature sintering of UN and U_3Si_2, making structural refinement possible. Additionally, atomistic simulations were, performed to quantify the thermodynamic stability of the proposed ternary phases.

2. Methods

2.1 Synthesis and Characterization of U-Si-N

The U_3Si_2 starting material has been prepared by arc-melting depleted uranium (dU) and silicon metal using a tri-arc furnace (5 TA Reed Tri Arc, Centorr Vacuum Industries, USA) equipped with a non-consumable 2% thoriated tungsten electrode and a water-cooled copper hearth under an atmosphere of high purity gettered argon. The surface of a depleted dU rod (99.9+% purity) was manually ground using a SiC grinding disc to remove the oxide layer and cleaned with acetone and methanol before being weighed. Chemical analysis on the uranium feedstock using Inductively Coupled Plasma–Mass Spectrometry (ICP-MS, MCL Inc.) revealed Co, Ni, and Cu impurities levels of 8.3, 2.6 and 2.7 ppm, respectively, with all other transition metal and rare earths impurities below detection limits. The mass of silicon metal (99.999% purity, Cerac, irregular shaped chunks, 3-6mm in size) was determined to achieve the targeted composition based on the mass of the uranium.

Small ingots of U_3Si_2 were arc melted under a gettered Ar-N_2 gas mixture of either 99% Ar - 1% N_2 (referred to as 1% N_2) or 90% Ar – 10% N_2 (referred to as 10% N_2). Due to the

oxidizing nature of uranium silicides, exceptional care was taken to ensure minimal oxygen contamination. All the arc melting processes were done inside an Ar atmosphere glovebox where the oxygen and water content were <0.1 ppm. The oxygen at the inlet and outlet of the arc melting furnace was measured to be less than 10^{-15} ppm before the start of each sample melt. For each of the samples, the ingot was melted five times, and turned over after each melt to ensure homogeneity. Additionally, molten titanium metal was maintained by use of an auxiliary electrode in a section of the arc-melter hearth to getter any residual oxygen.

Scanning electron microscopy (SEM) and X-ray diffraction (XRD) analysis were used to investigate the microstructure and phases present for each of the as-melted samples. A sample of the U_3Si_2 feedstock was characterized before the nitriding process to follow any microstructural change with N_2 composition. SEM samples were prepared by fracturing the ingots, potting samples in epoxy and grinding and polishing with SiC grinding discs with a 3-µm diamond suspension for the final polish. A Phenom ProX SEM equipped with a backscatter electron detector to obtain phase contrast images and energy dispersive spectrometer (EDS) was used for imaging and analyzing the samples. A Hitachi S-3400N with an OXFORD INCA wavelength dispersive electron probe microanalyser (EPMA) was also used for quantitative analysis of the phases compositions. Calibration was performed using Si_3N_4 (99.9%) as reference for Si and N. Measurements were performed at an acceleration voltage of 10kV at 35 nA on the faraday cup and employing spectrometer crystals TAP for the Si±Kα and LSM60 for N±Kα radiation.

XRD samples were prepared by grinding powders from ingot fragments using a mortar and pestle inside an Ar atmosphere glovebox. The powder was mounted on a Si crystal zero-background plate using a thin layer of vacuum grease and then O-ring sealed inside a polymer dome while inside the glovebox to reduce the risk of oxidation. The polymer dome had a scatter shield to minimize the background-to-signal noise. The XRD pattern was collected on a Bruker XRD (D2 Phaser, Bruker AXS, Madison, WI, USA), from 15° to 90° 2θ with a 5s hold and a 0.01° step size. Rietveld refinement was conducted using the MAUD software [26]. Structure models for the ternary phases in the analogous U-Si-C system were adopted: $U_{20}Si_{16}C_3$ (space group *P6/mmm*) and $U_3Si_2C_2$ (space group *I4/mmm*) [27] and their lattice parameters were used has initial values for the refinement.

2.2. Computational Methods: Atomic scale simulation

The Vienna Ab-initio Simulation Package (VASP) [28] was used to simulate the crystalline systems for UN, U_2N_3 (hexagonal), U_3Si_2, α-U and the candidate ternary phases $U_{20}Si_{16}N_3$ and $U_3Si_2N_2$. The electronic exchange and correlation energies were calculated within the generalized gradient approximation (GGA) in the Perdew-Burke-Ernzerhof (PBE) formalism [29]. The valence electrons explicitly treated in the calculations were $6s^26p^66d^25f^27s^2$ for U; $3s^23p^2$ for Si; and $2s^22p^3$ for N; with a plane wave expansion cut-off energy of 520 eV. An on-site Coulombic correction (GGA+*U*) method was applied using Dudarev's implementation [30] to predict the experimentally observed phases accurately: The U_{eff} values of 1.5eV for U_3Si_2 as used as in previous work [22] and 1.85 eV for UN, again from previous work [20] enabling the correct magnetic structure of the system to be predicted, and for $U_{20}Si_{16}N_3$ and $U_3Si_2C_2$ U_{eff} values of 0-2.9eV were systematically used to understand what effect the on-site Coulombic correction may have for on the relative stability as a value has not as yet been experimentally or theoretically verified. U_2N_3 was treated with the same parameters as UN.

To permit the comparison of compounds simulated with differing on-site Coulombic corrections, the single point energy of isolated uranium atoms with the various corrections were calculated and the difference in energy was used to correct the free energy of the various systems [31,32]. Single unit cell calculations were deemed suitable for all the calculations. The calculations were performed using an energy (electronic) and force convergence criterion of 10^{-5} eV and 0.02 eV/Å, respectively. A γ-centered Monkhorst-pack *k*-point grid was used for each system (8x8x8 for UN, 6x6x8 for U_3Si_2, 6x6x4 for $U_3Si_2N_2$ and 4x4x4 for the $U_{20}Si_{16}C_3$ and U_2N_3 unit cells)and Gaussian smearing of 0.2 eV was used for the calculations. During the relaxation, the volume, shape and symmetry of the cells were allowed to relax. The final structural symmetry reported was obtained from the FINDSYM [33] algorithm, using a tolerance of 0.05 Å. For the ternary structures, phonon analysis was performed using the code Phonopy [34] with the density functional perturbation theory (DFPT) formalism [35] enforcing their respective space group symmetry. Before running the phonon calculations, the primitive unit cells were relaxed using stricter energy and force convergence criteria, 10^{-8} eV and 0.001 eV/Å, respectively.

As noted above, the carbide and nitride systems of uranium are similar in many respects [36,37], and thus the ternary structures reported for the U-Si-C system were used to build the initial cells for the electronic calculations. The $U_{20}Si_{16}C_3$ structure has the *P6/mmm* symmetry: Uranium atoms occupy 1a (0.0, 0.0, 0.0), 1b (0.0, 0.0, 0.5), 6l (0.2152, 0.4304, 0.0), 6m (0.2126, 0.4252, 0.5) and 6i (0.5, 0.0, 0.2862) sites, silicon occupies the 4h (0.333, 0.666, 0.252) and 12n (0.229, 0.0, 0.246) sites and N occupies the 3f (0.5, 0.0, 0.0) site . The $U_3Si_2C_2$ structure has *I4/mmm* symmetry: Uranium atoms occupy the 2a (0.0, 0.0, 0.0) and 4e (0.0, 0.0, 0.266) sites, silicon occupies the 4e (0.0, 0.0, 0.408) site and nitrogen occupies the 4e (0.0, 0.0, 0.3058) site. The cells modeled in the present work are shown in **Figure 1**.

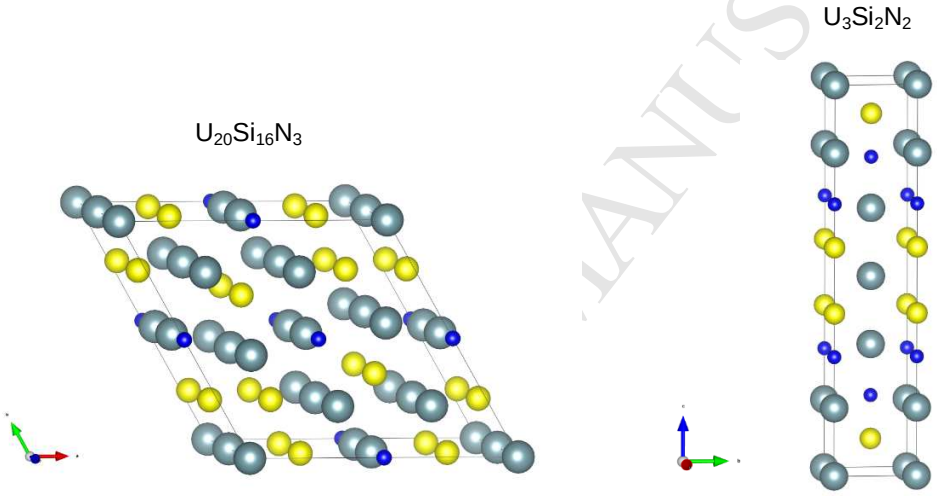

Figure 1: Structure of $U_{20}Si_{16}N_3$ and $U_3Si_2N_2$ modeled in this work. Uranium atoms (cyan), silicon (yellow), nitrogen (blue).

3. Results and Discussion

3.1. Tertiary U-Si-N phase formation

Figure 2 shows the microstructures of the initial U_3Si_2 material and that after re-arc melting under 1% and 10% N_2 atmosphere.

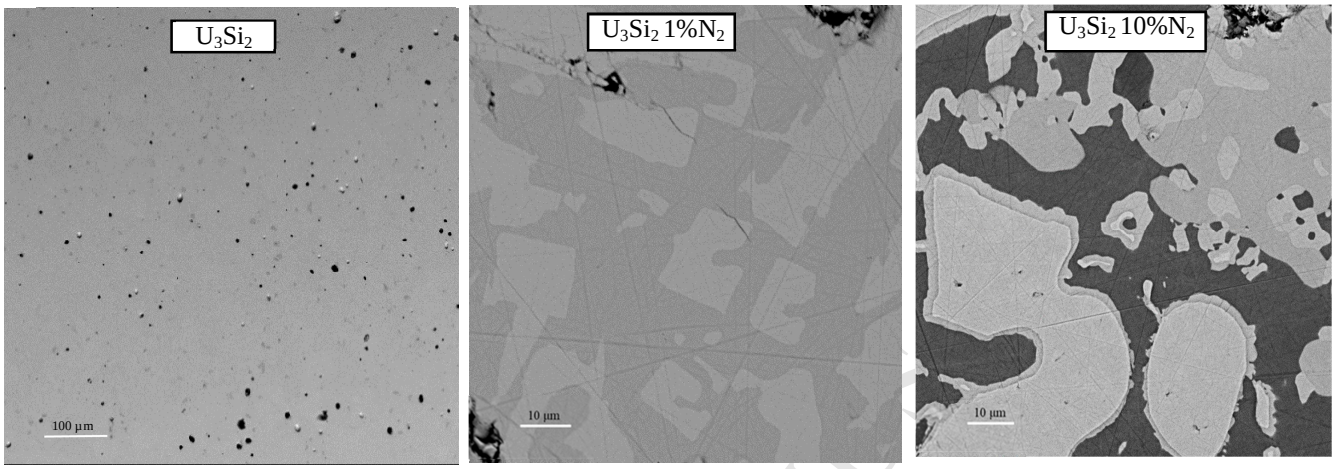

Figure 2: SEM images of (a) initial U_3Si_2 ingot and after nitriding under (b) 1% N_2 and (c) 10% N_2.

Both argon-nitrogen atmospheres resulted in a multi-phase material. The increase in the nitrogen concentration significantly changes the phase morphology. The sample arc-melted in 1% N_2 atmosphere resulted in a material composed of uranium-rich primary precipitates dispersed in a continuous matrix depleted of uranium as is apparent from phase contrast. The sample arc-melted in 10% N_2 shows a more complex microstructure, where three distinct phases can be observed. The large primary (uranium-rich) precipitates are observed surrounded by a layer of a phase with intermediate backscattering contrast. These phases are dispersed in a matrix depleted of uranium.

Figure 3 shows an EDS map for the sample arc-melted under 10% N_2. The primary phase is composed only of uranium and nitrogen. Its occurrence as the primary precipitate with a high melting point, and high uranium density is suggestive of a UN phase. The layer surrounding the UN precipitates contains U, Si and N (the latter at a small concentration), and thus associated with a ternary phase. Considering the observed microstructure, a mechanism of formation through a peritectic reaction [UN + silicide liquid → U-Si-N ternary] can be proposed. The matrix is composed only of U and Si, and its dark contrast, in comparison with the matrix

observed for the sample arc-melted in 1 % N_2, suggests the formation of a more silicon-rich phase such as USi.

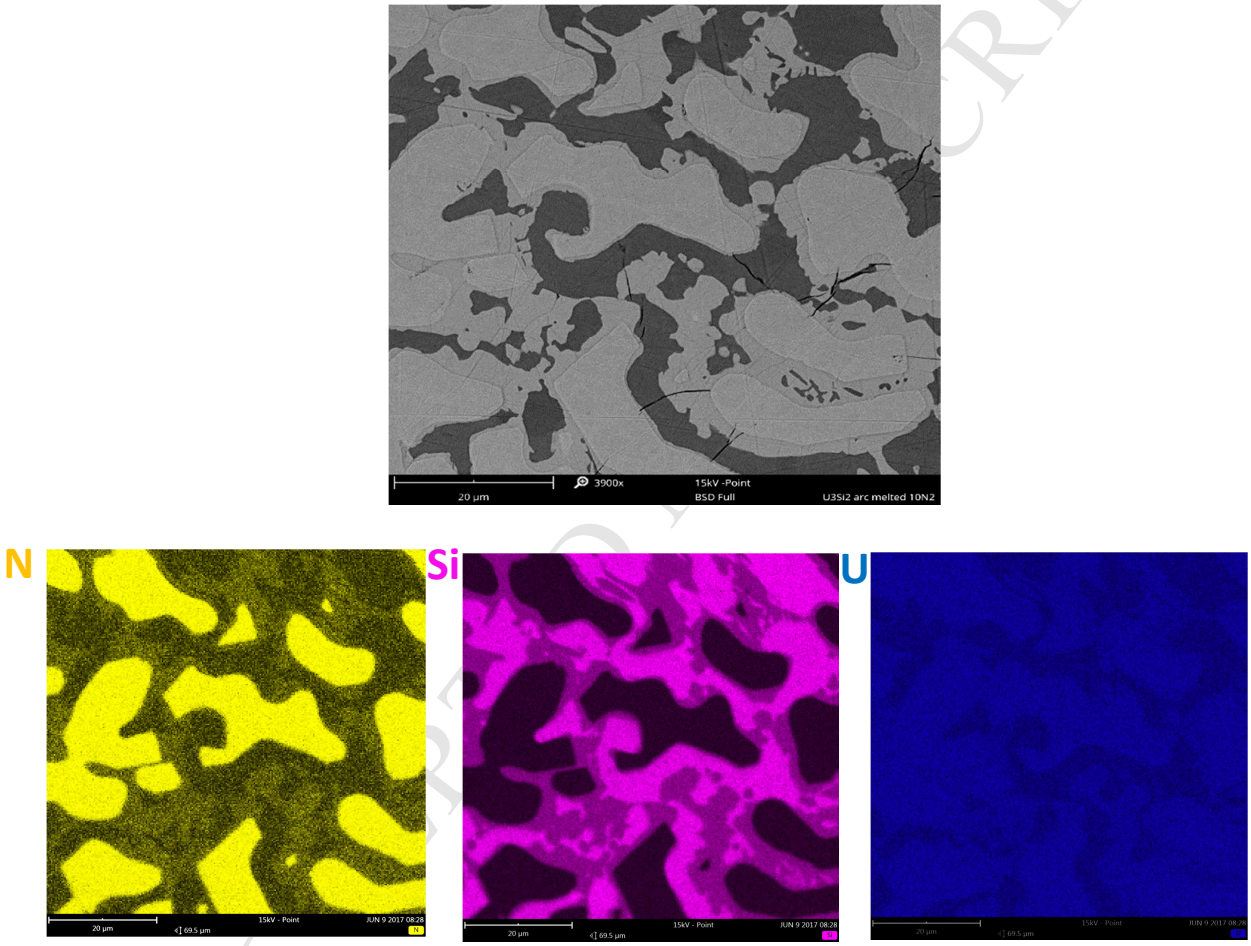

Figure 3: SEM-EDS map of sample nitrided under a 10% N_2 atmosphere.

The EPMA analysis reveals that there are two different ternary compositional areas. One rich in nitrogen with an average composition of U 51.3 at.% (±0.8), Si 39.3 at.% (±0.7), and N 9.4 at.% (±1.1), and a nitrogen depleted area with average composition of U 55.3 at.% (±0.7), Si 39.5

at.% (±0.6), and N 5.2 at.% (±1.0). The first possesses a composition close to the $U_{20}Si_{16}N_3$ phase. The second has a composition close to U_3Si_2 and may represent this phase with significant solubility for nitrogen. The dark matrix shows an average composition of U 49.2 at.% (±0.6), Si 48.9 at.% (±0.5) and N 1.8 at.% (±0.9), and thus possibly USi with little solubility for nitrogen in the phase. No composition close to $U_3Si_2N_2$ was observed.

Structural analysis of each type of sample was performed by XRD and the results are shown in **Fig. 4**. The initial material is confirmed to be composed of single-phase U_3Si_2 within the sensitivity of XRD, with good agreement with the powder diffraction file PDF 00-047-1070 [38]. The sample arc-melted in 1 % N_2 shows the presence of three distinct crystal structures; U_3Si_2 with a distorted cell (peaks shifted in comparison PDF-00-047-1070), UN (PDF 00-032-1997) [39] and the USi (PDF 01-075-1961) [40]. The sample arc-melted in 10% N_2 shows similar results with presence of distorted U_3Si_2, UN and USi phases, and three additional peaks at 26.085°, 29.638°, and 39.883° that could not be indexed. These extra peaks correspond to those reported by White *et al.* [15] which were associated with a ternary U-Si-N phase.

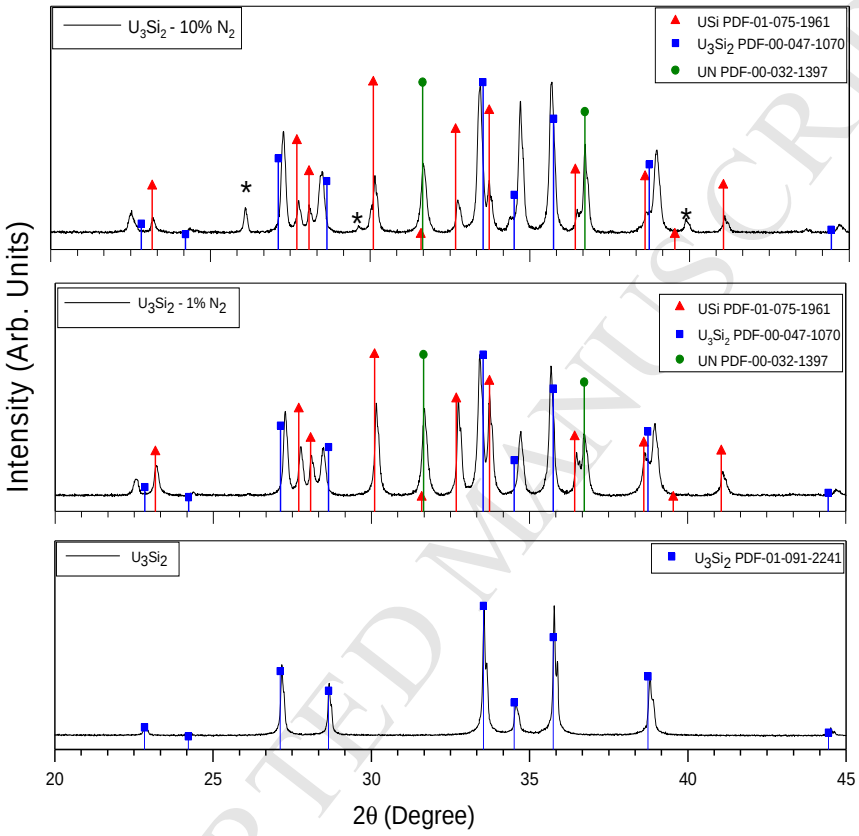

Figure 4: XRD patterns for U_3Si_2 ingots that were nitrided under 99% Ar - 1% N_2 and (b) 90% Ar – 10% N_2 indexed using PDF's of U_3Si_2 **[38]**, USi **[40]** and UN **[39].** * indicates peaks that did not match well with database values and likely correspond to an unknown U-Si-N phase.

Rietveld refinement was performed on patterns for all samples and the obtained lattice parameters are reported in **Table 1**. Both 1 % N_2 and 10% N_2 nitrided samples exhibit a distorted U_3Si_2 structure with an expansion of the *a* and *b* lattices of ~1%. As noted above, this may reflect the incorporation of nitrogen in the U_3Si_2 structure revealing some solubility, similar to the behavior reported in the U-Si-C system [27]. An slight expansion is also observed for UN which may indicate some presence so nitrogen defects or silicon incorporation.

For the sample arc-melted in 10% N_2 the experimental pattern could be well reproduced with a $U_{20}Si_{16}N_3$ structure, derived from the structure of the analogous $U_{20}Si_{16}C_3$ phase. The refined XRD pattern is shown in **Fig. 5** over the 15-60^o range. The consideration of $U_{20}Si_{16}N_3$ not only allows indexing of the three extra peaks, but accounts for observed overlapping and low intensity peaks (arrows in **Fig. 5**). The obtained lattice parameters for $U_{20}Si_{16}N_3$ are larger than those for the analogous U-Si-C phase which were used as initial values, reflecting the larger atomic radius of nitrogen as compared to carbon. In agreement with the microstructure analysis, no evidence of the structure $U_3Si_2N_2$ was observed in the XRD patters.

Table 1: Crystallographic values of samples nitrided in 1%N_2 and 10% N_2 compared to the starting material U_3Si_2. The values were obtained by Rietveld refinement using the MAUD [26] software.

Sample	**Phase**	**Space Group**	**Lattice parameters (Å)**	**R_{wp}**
U_3Si_2	U_3Si_2	*P4/mbm*	a=7.239 c = 3.905	0.0343
1 % N_2	U_3Si_2	*P4/mbm*	a=7.309 c=3.942	0.0541
	USi	*Pnma*	a=5.662 b=7.663 c=3.900	
	UN	*Fm-3m*	a=4.892	
10% N_2	U_3Si_2	*P4/mbm*	a=7.307 c=3.941	0.0703
	USi	*Pnma*	a=5.656 b=7.665 c=3.899	
	UN	*Fm-3m*	a=4.891	
	$U_{20}Si_{16}N_3$	*P6/mmm*	a=10.427 c=7.908	

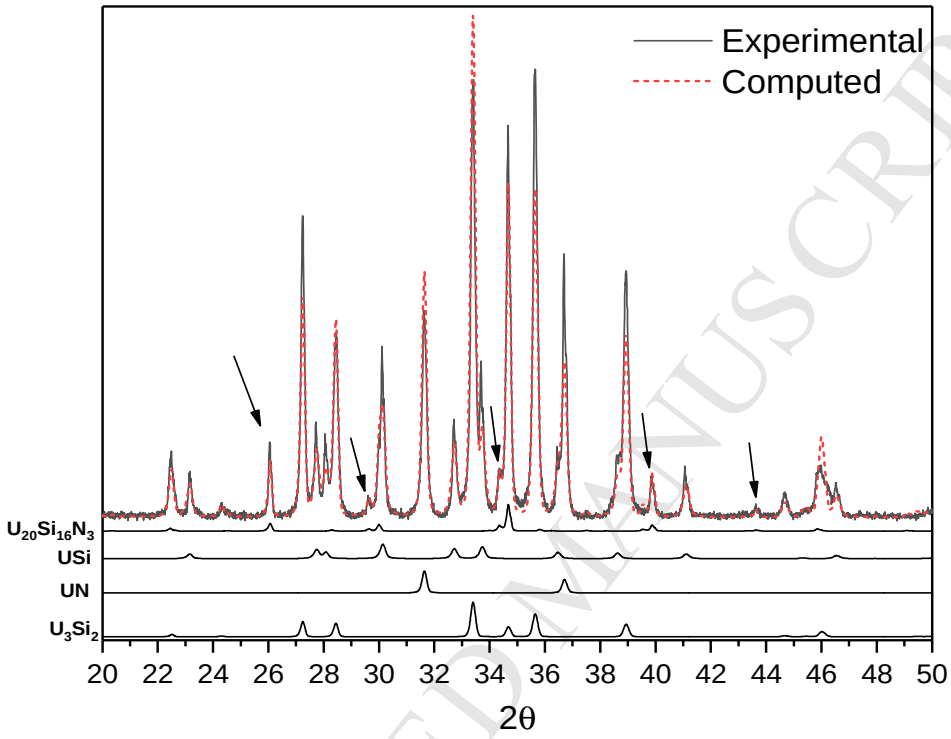

Figure 5: Rietveld refinement of a sample arc-melted 10% N_2 assuming a structure for $U_{20}Si_{16}N_3$. Arrows point out reflections that are associated with the ternary $U_{20}Si_{16}N_3$ structure.

The experimental results obtained in this work demonstrate the existence of a $U_{20}Si_{16}N_3$ ternary phase in the U-Si-N system. This ternary was found to coexist with U_3Si_2, UN and USi, validating the assumption of the similarity between the U-Si-N and U-Si-C systems. Even though there is no experimental evidences of the ternary phase $U_3Si_2N_2$, its stability should not be disregard, once its formation may be favored once the system has fully equilibrated. Therefore, it is worthwhile evaluating its stability by thermodynamic modeling methods, in order to assess the broader equilibria phase space in the U-Si-N system.

3.1. Computed thermodynamic stability of $U_{20}Si_{16}N_3$ and $U_3Si_2N_2$ phases

The lattice parameters obtained from structural optimization of $U_{20}Si_{16}N_3$ and $U_3Si_2N_2$ using varied U_{eff} values are shown in **Fig. 6**. For the $U_{20}Si_{16}N_3$ phase, all U_{eff} values from 0.3 eV to 1.9 eV produced a unit cell that had *P6/mmm* symmetry – the same symmetry used to refine the experimental XRD pattern. Lower U_{eff} values caused the unit cell to relax to a *P6/m* structure whilst higher U_{eff} values yielded a *P-3m1* or *P1* structure, disagreeing with our observations. The lattice parameters varied with the on-site Coulombic correction, increasing monotonically with the increment in the value of U_{eff} at values >0.9eV. The lattice parameter valuers in Fig. 6 for *a* and *b* close to U_{eff}=1.1 eV agree with our experimental observations, with the value for *c* being overestimated by approximately 2.6%. This result strongly supports the experimentally determined ternary structure.

The $U_3Si_2N_2$ structure does not preserve symmetry after relaxation for all U_{eff} values above 0.3 eV. The lattice constants for *a* and *c* were found to vary significantly with U_{eff} values up to 2.3 eV, above which a more consistent behavior was seen. This indicates that the electron correlation effect in this phase requires a larger Hubbard term, similar to that for $U_3Si_2C_2$ [24] due to the more complex electronic configuration resulting from the larger number of silicon and nitrogen bonds than present in $U_{20}Si_{16}N_3$ (see Fig. 1).

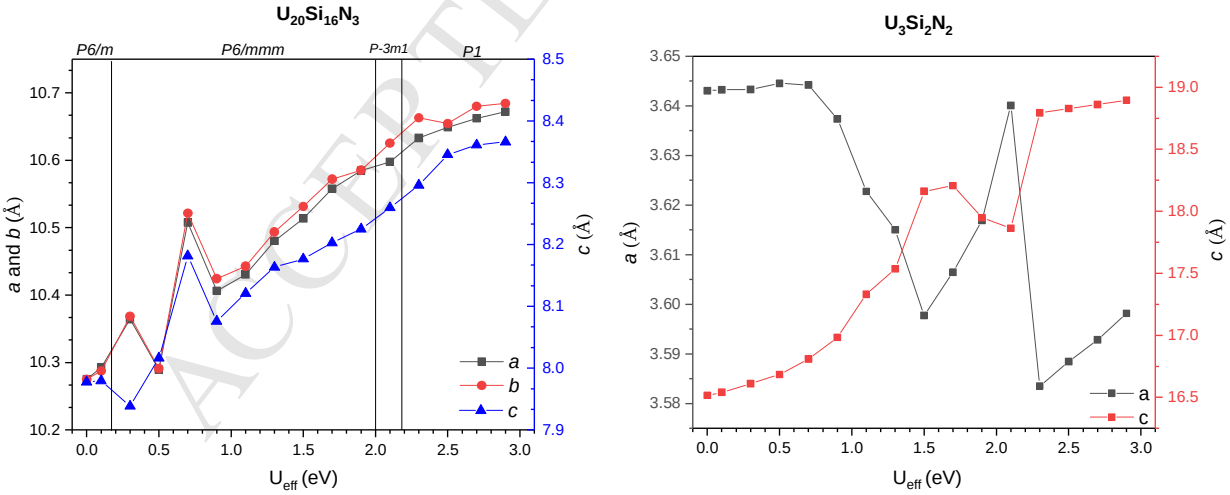

Figure 6: Lattice constants of $U_{20}Si_{16}N_3$ and $U_3Si_2N_2$ after structural optimization with varying on-site Coulombic corrections (U_{eff}). For $U_{20}Si_{16}N_3$ the computed structures s (with 0.05 Å tolerance) are also reported.

Two reactions were considered to investigate the relative stability of the proposed ternary phases; the reaction of U_3Si_2 with UN (equation 1 and 3), and that of U_3Si_2 with U_2N_3 (equation 2 and 4):

$$8U_3Si_2 + 3UN \rightarrow U_{20}Si_{16}N_3 + 7U \quad (1)$$

$$8U_3Si_2 + U_2N_3 \rightarrow U_{20}Si_{16}N_3 + 6U \quad (2)$$

$$U_3Si_2 + 2UN \rightarrow U_3Si_2N_2 + 2U \quad (3)$$

$$U_3Si_2 + {}^{2}/_{3}\,U_2N_3 \rightarrow U_3Si_2N_2 + {}^{4}/_{3}\,U \quad (4)$$

The relations allow only a narrow phase space to be evaluated compared to the full phase diagram. However, the determination of local minima is considered enough for the purpose of the present work.

The reaction enthalpies for all on-site Coulombic corrections (0-2.9 eV) for the formation of $U_{20}Si_{16}N_3$ and $U_3Si_2N_2$ are shown in **Fig. 7**.

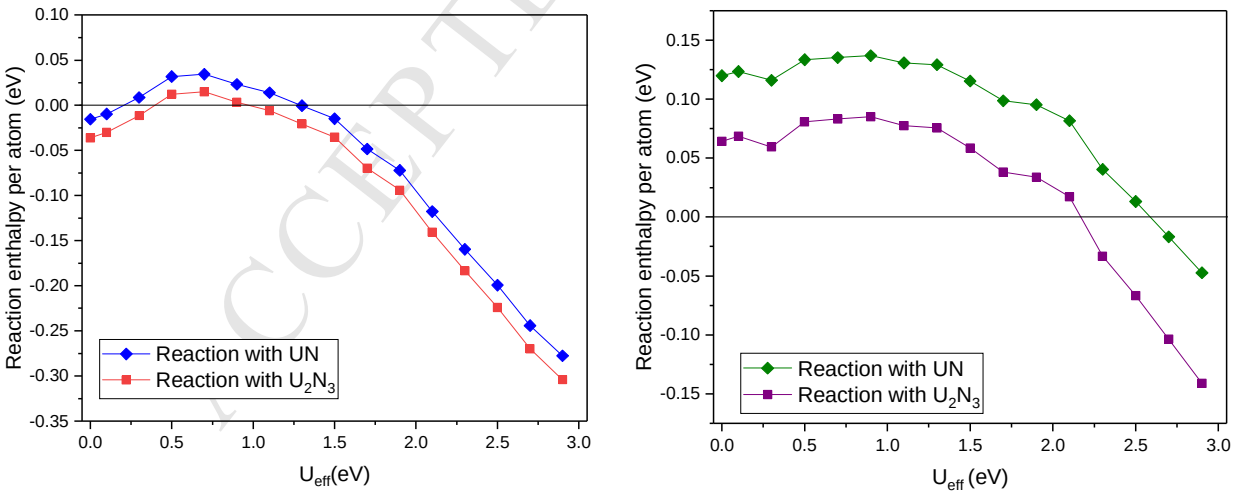

Figure 7: Reaction enthalpy (a) producing $U_{20}Si_{16}N_3$ from U_3Si_2 and UN (reaction given in equation Eq. 1) and U_2N_3 (Eq. 2) and (b) producing $U_3Si_2N_2$ from U_3Si_2 and UN (Eq. 3) and U_2N_3 (Eq. 4).

The $U_{20}Si_{16}N_3$ phase reactions (Eq. 1 and 2) are predicted to proceed exothermically for U_{eff} values below 0.3 eV and higher than 1.1 eV. Considering that the best agreement with the experimental crystal structure was observed around U_{eff}=1.1 eV, the $U_{20}Si_{16}N_3$ phase can be considered stable at this U_{eff} value. This result may suggest that this ternary phase can exist at lower temperatures in equilibrium with the sesquinitride meaning its formation at low temperature may be retarded by diffusion of species within the structure.

The reaction energies obtained for the $U_3Si_2N_2$ phase are less favorable compared to the $U_{20}Si_{16}N_3$. Unlike the $U_{20}Si_{16}N_3$ phase, the reactions provide positive formation enthalpies (i.e., they are not predicted to proceed exothermically) for U_{eff} values up to 2.1 eV and 2.5 eV with U_2N_3 and UN, respectively. Although there are no experimental lattice parameters which fit U_{eff} values, and that a higher correlation factor of U_{eff}=4.0 eV is required for $U_3Si_2C_2$ [24], while less likely, the existence of a $U_3Si_2N_2$ ternary phase cannot be ruled out.

To further ascertain dynamical stabilities, the phonon density of states of the ternary phases were calculated for U_{eff} = 1.1eV and the results are shown in **Fig. 8.**

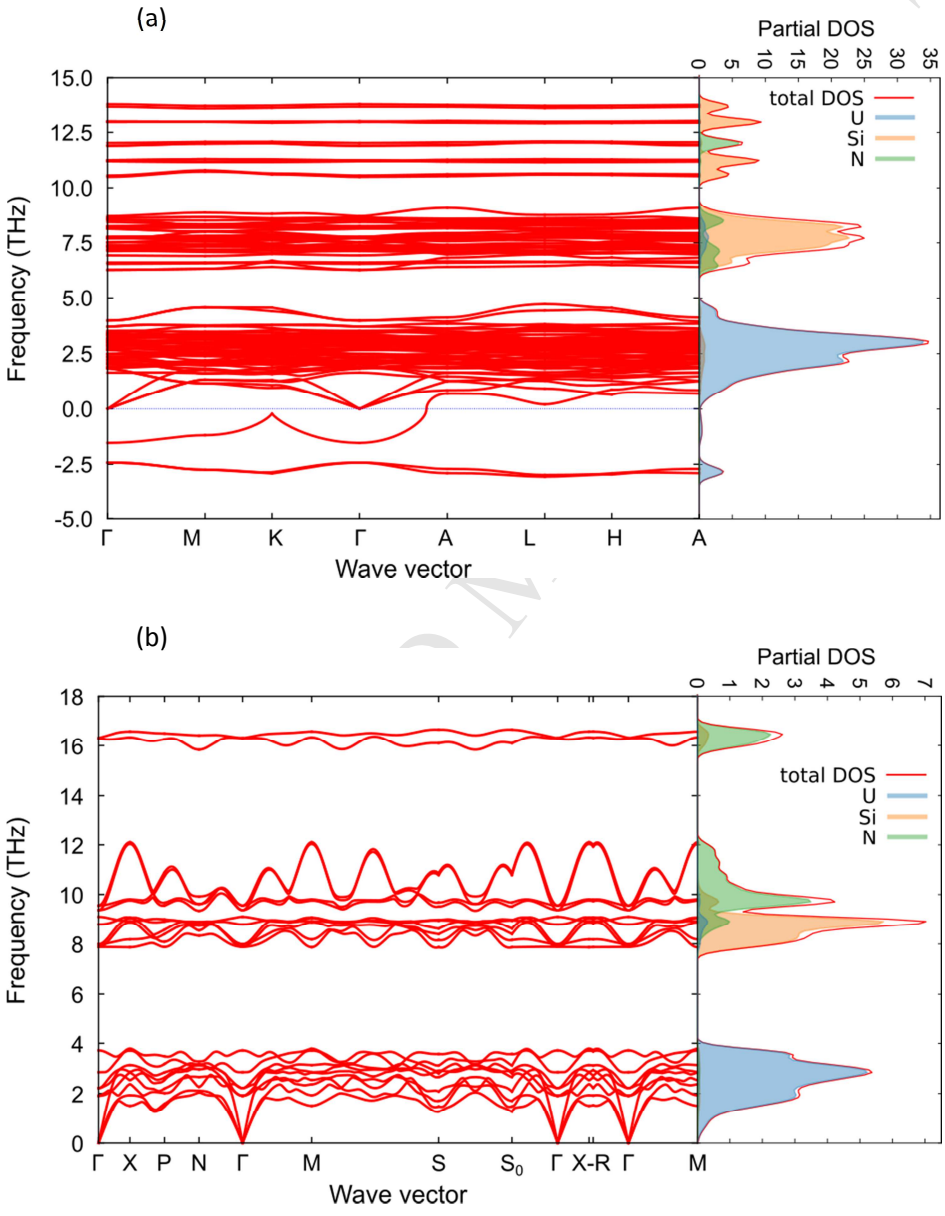

Figure 8: Phonon dispersion and partial phonon density of states (PDOS) for (a) $U_{20}Si_{16}N_3$ (*P6/mmm*) and (b) $U_3Si_2N_2$ (*I4/mmm)* using GGA+*U* with U_{eff}=1.1eV. The PDOS of U, Si, N and the total DOS are shown in blue, orange, green and red, respectively.

As shown in **Fig.8b,** the absence of imaginary phonon frequencies in the $U_3Si_2N_2$ phonon dispersion indicates that the considered structure is dynamically stable at 0 K. However, imaginary phonon frequencies were obtained for the $U_{20}Si_{16}N_3$, associated exclusively with the uranium atoms (see partial DOS in **Fig. 8a**), suggesting a dynamical instability of this phase at 0 K, which does not exclude the possibility of this phase being stable at higher temperatures. Analyzing the on-site force constants eigenvalues, $\Phi(0,0)$, showed that the uranium atoms have a single minimum (all eigenvalues are positive), meaning the $U_{20}Si_{16}N_3$ phase can be stabilized by anharmonic and thermal fluctuations at temperatures higher than 0 K. To further analyze the displacement caused by the negative frequencies, we generated structures with displacements along each of the negative phonon modes, and the resulting structures are shown in **Fig. 9,** where the displacements are made apparent using translucent spheres. It is apparent that the displacements are symmetric with respect to the equilibrium uranium positions, resembling thermal fluctuations and do not create any net shear that would otherwise destabilize the structure. These types of distortions are difficult to detect in XRD as positions are indicated by the average electron density. Thus, there is confidence in the stability of the $U_{20}Si_{16}N_3$ phase at T > 0 K, but the uranium atoms may not be located in the exact positions described by the *P6/mmm* space group, meaning the experimentally observation is a result of the average uranium atom positions. It is also important to mention that entropic contributions can overcome the impact of the negative frequencies, reducing their influence at T > 0 K. It is worth noting that incorporating nitrogen atoms at the interstitial site of the analogous U_5Si_4 phase stabilizes the negative phonon frequencies otherwise seen in the phonon dispersion of the U_5Si_4 [41]. We should also point out that there is a possibility of the relaxed structure being in a meta-stable state, a known issue with DFT+*U* method when occupational matrix is not a priory specified [42], which might cause the dynamical instability. While the results for 0 K indicate a more stable structure for $U_{20}Si_{16}N_3$ should exist at that temperature, determining that structure is computationally prohibitive mainly because of the expensive phonon calculations required to verify that structures relaxed using different occupational matrices are dynamically stable.

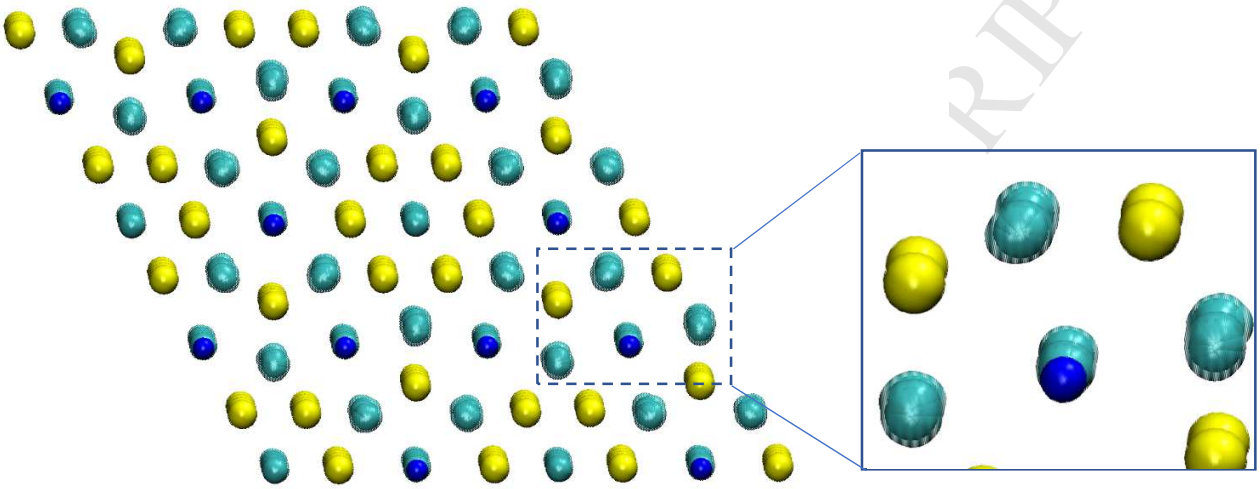

Figure 9: Symmetric $U_{20}Si_{16}N$ (*P6/mmm*) structures overlapping illustrating the displacement caused by imaginary phonon frequencies displayed as translucent spheres. Uranium (cyan), Silicon (yellow), Nitrogen (blue).

4. Conclusions

Ternary phase-containing samples in the U-Si-N system were fabricated by arc-melting U_3Si_2 in an argon-nitrogen atmosphere. A mixture of Ar-10% N_2 was sufficient for ternary phase formation that possessed a distinct crystallographic lattice. Rietveld refinement allowed the phase to be identified as $U_{20}Si_{16}N_3$ with the space group *P6/mmm*, demonstrating its similarity to the U-Si-C system. First principles calculations in the DFT+*U* formalism were performed to

further investigate the stability of the nitride analogues to the ternary phases in the U-Si-C system, $U_{20}Si_{16}N_3$ and $U_3Si_2N_2$. $U_{20}Si_{16}N_3$ was found to be energetically favored in formation from U_3Si_2 reacting with UN or U_2N_3 for value U_{eff} values of ~1.1 eV. This value also produced lattice parameters very close to those observed experimentally. The $U_3Si_2N_2$ phase is computed to be energetically stable for high U_{eff} values (2.1eV-2.5eV), and was found to be dynamically stable at 0 K. Although $U_{20}Si_{16}N_3$ exhibits some computed imaginary phonon frequencies for the uranium atoms, it was demonstrated that these phonons only generate small distortions in the unit cell, resembling thermal fluctuations. Thus there is confidence in the stability of the $U_{20}Si_{16}N_3$ phase in the U-Si-N system.

5. Acknowledgments

This research is being performed using funding received from the DOE Office of Nuclear Energy's Nuclear Energy University Programs. The authors wish to thank Mr George Wetzel at the Clemson University Electron Microscopy Laboratory for operation and use of their Hitachi S-3400N SEM. This work used the Extreme Science and Engineering Discovery Environment (XSEDE), which is supported by National Science Foundation grant number ACI-1548562, the Beskow and the HPC cluster Hyperion, supported by The Division of Information Technology at University of South Carolina.

References

[1] M. Braun, “The fukushima daiichi incident," AREVA Report. Available online: http://www.wdr.de/tv/monitor//sendungen/2011/0407/pdf/areva-fukushima-report.pdf , 2011.

[2] IAEA, “Benchmark study of the accident at the fukushima daiichi nuclear power plant," Tech. rep., OECD/NEA, February 2016.

[3] J. Bischoff, P. Blanpain, J-C. Brachet, C. Lorrette, A. Ambard, J. Strumpell, K. McKoy, Development of Fuels with enhanced accident tolerance, Accident Tolerant Fuel Concepts for

Light Water Reactors, IAEA Tecdoc 1797, (2014) 22-29.

[4] S. Zinkle, K. Terrani, J. Gehin, L. Ott, and L. Snead, J. Nucl. Mater.448 (2014) 374–379.

[5] B. Pint, K. Terrani, T. Yamamoto and L. Snead, Metall. Trans. E 2 (2015) 190-196.

[6] Westinghouse Electric Company, Development of LWR Fuels with Enhanced Accident Tolerance, Final Technical Report (2015).

[7] Y. Arai, Nitride fuel, in: R. Konings (Ed.), Comprehensive Nuclear Materials, vol. 3, Elsevier Ltd, 2012, pp. 41-53.

[8] S. Hayes, J. Thomas, and K. Peddicord, J. Nucl. Mater. 171 (1990) 300–318.

[9] R. Metroka, “Fabrication of uranium mononitride compacts,” tech.rep., NASA, July 1970.

[10] G. Youinou and R. Sonat Sen, “Enhanced accident tolerant fuels for lwrs - a preliminary system analysis,” tech. rep., INL, September 2013.

[11] J. Snelgrove, R. Domagala, G. Hofman, and T. Wiencek, “The use of u3si2 dispersed in aluminum in plate- type fuel elements for research and test reactors,” tech. rep., Argonne National Laboratory, October 1987.

[12] J. White, A. Nelson, J. Dunwoody, D. Byler, D. Safarik, K. McClellan, J. Nucl. Mater. 464 (2015) 275-280.

[13] E. Sooby Wood, J. White, C. Grote, A. Nelson J. Nucl. Mater. 501 (2018) 404-412.

[14] A. T. Nelson, A. Migdissov, E. Sooby Wood, and C. Grote, J. Nucl. Mater. 500 (2018) 81-91.

[15] J. T. White, A. W. Travis, J. T. Dunwoody, A. T. Nelson, J. Nucl. Mater. 495 (2017) 463-474.

[16] K. D. Johnson, A. M. Rafter, D. A. Lopes, J. Wallenius, J. Nucl. Mater. 477 (2016) 18-23.

[17] L. Ortega, B. Blamer, J. Evans, and S. McDeavitt, J. Nucl. Mater. 471 (2016) 116–121.

[18] J. Hammond, "Process for sintering uranium nitride with a sintering aid depressant," US Patent, October 1965.

[19] D.A. Lopes, S. Uygur, K. Johnson, J. Nucl. Sci. Technol. 54 (2017) 405-413.

[20] D. Gryaznov, E. Heifets, E. Kotomin. Phys. Chem. Chem. Phys. 14 (13) (2012) 4482-4490.

[21] A. Claisse, M. Klipfel, N. Lindboma, M. Freyss, P. Olsson. J. Nucl. Mater. 478 (2016) 119–124.

[22] M. Noordhoek, T. Besmann, D. Andersson, S. Middleburgh and A. Chernatynskiy, J. Nucl. Mater. 479 (2016) 216-223.

[23] Nicolas Brisset. Etude physico-chimique et des propriétés électroniques de composés uranifères binaires et ternaires dans les systèmes U-Si-B et U-Pt-Si. Autre. Université Rennes 1, 2016. Français. <NNT :2016REN1S135>. <tel-01576696>.

[24] S.F.Matar R.Pöttgen. Chem. Phys. Lett. 550 (2012) 88–93.

[25] R. Endebrock, E. Foster Jr., and D. Keller, "Preparation and properties of cast un," tech. rep., Battelle Memorial Institute, 1964.

[26] Lutterotti L, Bortolotti M, Ischia G, Lonardelli I. Wenk HR. Rietveld texture analysis from diffraction images. Z. Kristallogr, Suppl. 26, (2007) 125-130.

[27] Noël H, Chatain S, Alpettaz T, Guéneau C, Duguay C, Léchelle J, " Experimental Determination of (U-Si-C) ternary phase diagram at 1000 °C and Experimental points in the quaternary (U-Pu-Si-C) system " F-Bridge Report -D-151-Rev, 2012.

[28] G. Kresse and J. Hafner, Phys. Rev. B 47 (1993) 558-561.

[29] J. P. Perdew, K. Burke, M. Ernzerhof, Generalized Gradient Approximation Made Simple, Phys. Rev. Lett. 77 (1996) 3865-3868.

[30] S. Dudarev, G. Botton, S. Savrasov, C. Humphreys and A. Sutton, Phys. Rev. B 57 (1998) 1505-1509.

[31] D. Bocharov, D. Gryaznov, Y. Zhukovskii and E. Kotomin, Surf. Sci. 605 (2011) 396-400.

[32] M. Klipfel and P. Van Uffelen, J. Nucl. Mater. 422 (2012) 137-142.

[33] H. T. Stokes and D. M. Hatch, J. Appl. Cryst. 38 (2005) 237-238.

[34] A. Togo, F. Oba, I. Tanaka, Phys. Rev. B 78 (2008) 134106.

[35] X. Gonze, C. Lee, Phys. Rev. B 55 (1997) 10355-10368.

[36] J. Williams and R. Sambell, J. Less Common Met. 1 (1959) 217-226.

[37] R. Rundle, N. Baenziger, A. Wilson and R. McDonald, J. Am. Chem. Soc. 70 (1948) 99-105.

[38] K. Remschnig, T. Le Bihan, H. Noel, P. Rogl, J. Solid State Chem. 97 (1992) 391-399.

[39] M.C. Morris, H.F. McMurdie, E.H. Evans, B. Paretzkin, H.S. Parker, N.C. Panagiotopoulos, Standard x-ray diffraction powder patterns, Section 18, in: C. Hubbard (Ed.), National Bureau of Standards Monograph, vol. 25U.S.Department of Commerce, 1981, p. 75.

[40] H. Vaugoyeau, L. Lombard, J. Morlevat, J. Nucl. Mater. 39 (1971) 323-329.

[41] D.A. Lopes, V. Kocevski, T. L. Wilson, E. E. Moore, T. M. Besmann J. Nucl. Mater. 510 331-336.

[42] B. Dorado, B. Amadon, M. Freyss, M. Bertolus, Phys. Rev. B 79 (2009) 235125.